ACS APPLIED MATERIALS & INTERFACES

Research Article

www.acsami.org

Effect of Humidity on Nanoparticle-Based Chemiresistors: A Comparison between Synthetic and Real-World Samples

Gady Konvalina and Hossam Haick*

The Department of Chemical Engineering and Russell Berrie Nanotechnology Institute, Technion − Israel Institute of Technology, Haifa 32000, Israel

ABSTRACT: Chemiresistors based on metal monolayer-capped nanoparticles (MCNPs) are promising candidates for fast, inexpensive, and portable tracing of (bio)chemical species in the gas phase. However, the sensitivity of such sensors to humidity is problematic, limiting their reliable and reproducible application in real-world environmental conditions. In this work, we employed a compensation method to explore the effect of humidity on a single MCNP chemiresistor as well as on an array of MCNP sensors used to analyze either synthetic or real-world samples. We show that an array of MCNP chemiresistors is able to precisely detect and estimate subtle concentrations of (mixtures of) volatile organic compounds (VOCs) under variable backgrounds of 2−83% relative humidity (RH) only after humidity compensation. Humidity effects were also tested in two clinical trials aimed at detecting prostate cancer and breast cancer through exhaled breath analysis. Analysis of the results showed improved cancer detection capabilities as a result of RH compensation, though less substantial than the impact of RH compensation on synthetic samples. This outcome is attributed to one − or a combination − of the following effects: (i) the RH variance was smaller in the breath samples than that in the synthetic samples; (ii) the VOC composition in the breath samples is less controlled than the synthetic samples; and (iii) the responses to small polar VOCs and water are not necessarily additive in breath samples. Ultimately, the results presented here could assist the development of a cost-effective, low-power method for widespread detection of VOCs in real-world applications, such as breath analysis, as well as for environmental, security, and food applications.

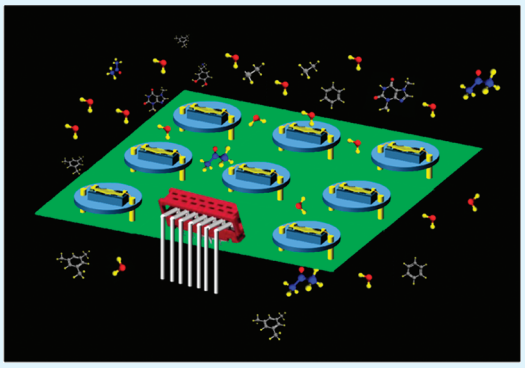

KEYWORDS: *nanoparticle, chemiresistor, humidity, compensation, drift, breath analysis, volatile organic compound*

INTRODUCTION

Chemiresistors based on metal monolayer-capped nanoparticles (MCNPs) hold promising potential for tracing volatile organic compounds (VOCs) in a wide variety of applications. This could be attributed to the MCNP sensors' controllable selectivity, high sensitivity, low detection limits, fast response and recovery times, small size, low-output impedance, and easy integration with standard microelectronic devices.[1−4]

Interaction of MCNP films with VOCs can have two counteracting effects: (i) film swelling/aggregation, which may increase/decrease the resistivity due to an increase in the interparticle tunnel distance; and/or (ii) an increase in the permittivity of the organic matrix around the metal cores that may decrease the resistivity because of a decrease in the activation energy and due to a reduction of the potential barrier height between the metal cores, which in turn decreases the tunneling decay constant.[1−3,5,6] However, the interaction of MCNP-based sensors with VOCs in real-world applications is hindered by the high and/or nonconstant humidity levels present in the environment and/or detected sample.[7−9] For example, a method for screening, diagnosis, and monitoring of cancer relies on the analysis of breath samples.[10,11] Yet the high relative humidity (RH) in the breath samples (>80% RH − equivalent to >25 000 ppm of water vapor at 1 atm and 25 °C) usually screens the cancer-related VOCs,[12−14] limiting the accuracy of the analysis.[10,15,16] This limitation is made more serious if the MCNP-based sensor drifts over time, due to, for example, aging, and/or incomplete release of absorbed chemical species.[17] Dehumidification and/or VOC preconcentration techniques can, in principle, be used to minimize the humidity effect.[16,18,19] However, these methods are costly, complex, and lose important VOCs during the extraction process of the compounds from the sample. Moreover, these techniques do not compensate for the sensor drift and the response to the remaining water vapor.

Synthesis of MCNPs with low sensitivity to humidity and increased VOC/humidity sensitivity ratio has been reported[9,20,21] (see also refs 16 and 22−25 for related work on other nanomaterial types). Garg et al. have shown that the long-term drift of chemiresistors based on Au MCNPs can be reduced by capping the nanoparticles with trithiols instead of monothiols, which presumably slows down the oxidation of the surface thiolates.[26] Nevertheless, this approach was demonstrated only with toluene. Guo et al.[8] have found short-term drift and signal

Received: October 6, 2011
Accepted: November 28, 2011
Published: November 28, 2011

distortion (especially at high RHs) phenomena to be related to residual ionic impurities, originating from the phase-transfer reagent tetraoctylammonium bromide (TOAB). These effects were eliminated by introducing a purification process after nanoparticle synthesis, to extract the ionic impurities, giving stable responses to VOCs and well-defined signals to water vapor from low to high RHs (80%). The well-defined signals to water vapor are particularly important as they enable VOC sensing in humid environments and make humidity compensation potentially possible.

Low sensitivity to water was reported for Au or Pt MCNPs deposited using the layer-by-layer technique.[9] These films exhibited water sensitivity on the order of $2-6 \times 10^{-5}$ percent response per ppm change of water vapor (%Res./ppm_w).[9] Dovgolevsky et al.[20] demonstrated that controlling the shape of Pt MCNPs to form cubic instead of spherical cores increases their sensitivity to VOCs by up to ten times. The reported sensitivity to water was on the order of $1-6 \times 10^{-4}$ %Res./ppm_w, while the sensitivity to a variety of VOCs was 2−400 times higher and the corresponding VOC/humidity sensitivity ratios ranged up to 1.3% RH/ppm_{voc}.[21] These results indicate that even sensors with sensitivities 400 times higher to VOCs than to water could be subject to significant response variations due to small humidity fluctuations of ∼1% RH when sensing low VOC concentrations (ppms or lower). Consequently, it is important to understand and quantify the potential humidity effects on VOC sensing using MCNP chemiresistors.

In this study, we investigate the effect of humidity on MCNP chemiresistors, both in lab applications and in real-world applications. We do so by exploring the efficiency of compensating the humidity effect: (i) in synthetic air/VOC/water mixtures during investigations carried out over short (1 week) and long (4 months) periods of time, and (ii) in real-world breath samples collected from patients with prostate cancer (PC) or breast cancer (BC) compared to healthy controls. We show that the efficiency of humidity compensation in synthetic samples is better than in real-world samples. We attribute this to the high RH variance and controlled VOC composition generated in the synthetic samples as well as to the reported additive nature of the MCNP sensor responses to humidity and the VOCs studied.

EXPERIMENTAL SECTION

Fabrication of Sensors. Monolayer-capped nanoparticles (MCNPs) consisting of 3−5 nm Au nanoparticles and dodecanethiol, octadecanethiol, 2-nitro-4-(trifluoromethyl)benzenethiol (NTFB), 2-mercaptobenzoxazole (MBA), 4-methoxy-α-toluenethiol (MTT), hexanthiol, *tert*-dodecanethiol, 2-ethylhexanethiol, 2-mercaptobenzyl alcohol, 3-methyl-1-butanethiol, butanethiol, or octadecylamine ligands were synthesized using a two-step seed-mediated growth method.[27] MCNP films were drop casted on circular interdigitated electrodes (5 mm diameter and 25 μm electrode width and spacing) fabricated by evaporating 50 nm of Ti followed by 350 nm of Au on Si wafers with a thermal oxide capping layer of 0.5 μm using conventional microfabrication processes. The MCNP sensors were left in a vacuum oven at 1 Torr and 50 °C overnight (or longer, until their resistance at ambient conditions stabilized). All organic reagents and chemicals employed in the MCNP synthesis were analytical grade materials obtained from Sigma-Aldrich, Israel.

Sensor Characterization in Laboratory Environment. The MCNP chemiresistors were exposed to various mixtures of water vapor (produced by vaporizing 18.2 MΩ cm DI water) and *n*-octane, as a representative example of a nonpolar VOC, 2-ethylhexanol (EH), as a representative example of a polar VOC, or 1,2,4-trimethylbenzene (TMB), as a representative example for an aromatic polar VOC. The three VOCs used in the current study (>98% purity, Sigma-Aldrich, Israel), resemble part of the VOCs appearing in exhaled breath samples. The mixtures were produced from a commercial dynamic liquid injection dilution (DLID) system (Umwelttechnik MCZ, Germany). Purified dry air (1.6−2.2% RH; <0.4 ppm VOC content) from a commercial zero-air system (NGA 600−25 MD, Umwelttechnik MCZ, Germany) was used as a carrier gas. The DLID system mixes a constant flow (100 ± 1 cm^3/min) of purified air with a constant mass flow source of vaporized VOC(s). The air/VOC mixture exiting the DLID system is then diluted with two flow controlled dilution air streams: (i) dry air obtained directly from the zero-air system, and (ii) humidified air generated by the system's humidifier module. The total output VOC concentration was determined by controlling the mass flow rate of the vaporized VOC(s) and the total volumetric air flow rate. The DLID system output VOC(s) concentration and RH were monitored by a commercial photoionization detector (PID; ppbRAE 3000) and a commercial RH sensor (Hygrosens), respectively. The sensing experiments were carried out by monitoring the MCNP sensors and environmental sensors (RH, temperature and pressure sensors), placed inside a 330 cm^3 stainless steel chamber, while exposed to the (mixtures of) compounds generated by the DLID system. A Keithley data logger device (model 2701 DMM) controlled by a custom Labview program was used to sequentially acquire resistance readings from the sensor array and voltage readings from the environmental sensors. Constant currents in the range of $0.7-1 \times 10^4$ μA were used for resistance measurements. A typical exposure cycle involved a 5 min vacuum (<50 mtorr) baseline step, followed by 5 min exposure to the test vapor under stagnant conditions, and ended with another 5 min vacuum step, whereas each successive acquisition cycle of the entire sensor array was completed in <4 s.

Clinical Samples. Breath samples were collected from patients having prostate cancer (PC), breast cancer (BC), and healthy controls in two separate clinical trials. The PC trial involved 16 breath samples from 9 diagnosed PC patients and 16 breath samples from 10 healthy subjects, aged 44−73. The breath samples of this trial were collected in the Oncology Division of the Rambam Health Care Campus (Haifa, Israel). The BC trial involved 20 breath samples from 10 diagnosed BC patients and 21 breath samples from 11 healthy subjects, aged 33−68. The breath samples of this trial were collected in the Breast Imaging Division of the Rambam Health Care Campus (Haifa, Israel).

Table 1. Clinical Characteristics of the PC, BC, and Control Population Groups

	PC	controls (PC)[a]	BC	controls (BC)[a]
subjects (*n*)	9	10	10	11
age (mean/1SD, years)	66/5	57/9	50/11	58/8
sex (male/female)	9/0	5/5	0/10	6/5
smokers	1	2	1	2

[a]Control samples for PC and BC clinical trials were collected during different periods, therefore they are not combined in the table.

The clinical characteristics of the subject groups are listed in Table 1. Due to the particular characteristics of these two diseases, the PC group included only males, whereas the BC group included only females. In any case, the output of the MCNP sensor array has not shown any statistical differences between the male and female populations of the two control groups (not shown) and between the upper and lower age spans within each of the four groups, in agreement with previous observations.[28,29]

Alveolar breath samples were collected into 750 cm^3 Mylar breath collection bags using a specially designed custom breath collection device, as described elsewhere.[28,30] The volunteers did not ingest alcohol for at least 12 h previous to their alveolar breath collection. Breath samples from the PC patients and the BC patients were

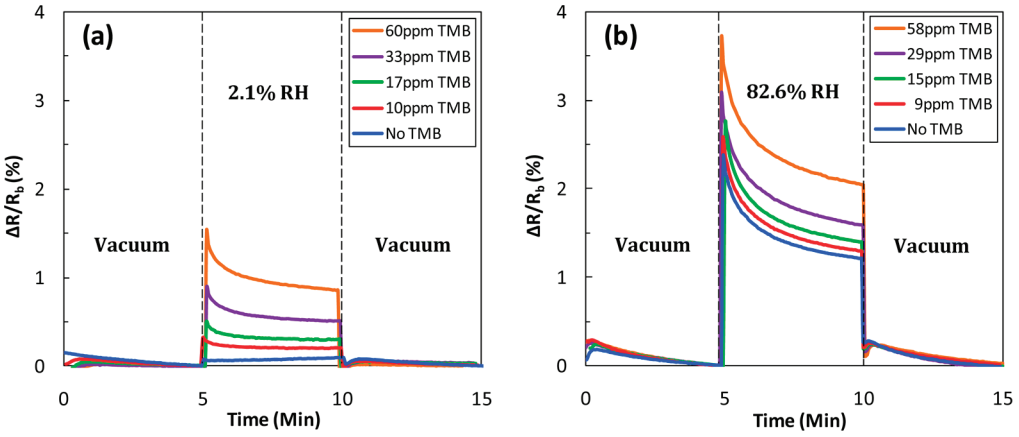

Figure 1. Dodecanethiol-Au MCNP chemiresistor response to increasing concentrations of TMB, with background RHs of (a) 2.1 ± 0.4% and (b) 82.6 ± 1.3%. TMB concentrations measured are depicted in the plot legends.

collected directly after the diagnosis and before any treatment. Three successive breath bags were collected from each subject; two were analyzed using the MCNP sensor array described in the "Fabrication of Sensors" part of the Experimental Section, and the third using a gas chromatography mass spectrometry (GC-MS) system via a solid-phase microextraction (SPME) fiber, as described elsewhere.[28] The sensor array measurements were performed following the same procedure specified in the "Sensor Characterization in Laboratory Environment" part of the Experimental Section. During the experiments, the test chamber and the breath bags were maintained at room temperature (25 ± 3 °C). To ensure sufficient sample volume, we monitored the in-chamber pressure during the breath sample exposures to be above 710 mmHg, with the upper margin being the barometric pressure (~760 mmHg).

Data Analysis. Analysis of sensing signals, extraction of response features, and development of humidity compensation methods were performed by Matlab (version R1010a, the MathWorks, Inc.) and JMP software (version 8.0, SAS Institute Inc.). Principal component analysis (PCA) was used to reduce data dimensionality and allow a better visualization of the multidimensional data sets. PCA defines new orthogonal axes, called principal components (PCs), which are linear combinations of the original data that capture the most variance from the whole data set, so that the multidimensional data can be represented in two or three dimensions only. The largest response variance can be found along PC1, with decreasing magnitudes of variance found along PC2, PC3 etc.[28] Discriminant factor analysis (DFA), which is a supervised linear method, was used to evaluate the effect of humidity compensation on the discriminative potential of the tested sensor arrays. The accuracy of VOC classification is calculated employing a leave-one-out cross-validation method. Given n measurements, DFA is computed n times using n-1 training vectors. The vector left out during the training phase (validation vector that is unseen by the DFA method during the training phase, thus completely new for the DFA model built) is then projected onto the DFA model built, which produces a classification result. The classification accuracy is estimated as the averaged possible performance over the n tests. The Partial Least Squares (PLS) method was used to estimate the effects of the humidity compensation on the correctness of VOC concentration estimation.[31]

RESULTS

Humidity Effect on the Sensing Characteristics of VOCs. Figure 1 shows normalized resistance responses ($\Delta R/R_b$, where ΔR is the resistance change after exposure to the test sample, and R_b is the baseline resistance before exposure) of a dodecanethiol-Au MCNP sensor exposed to air with various concentrations of TMB and with a RH of: (a) 2.1 ± 0.4% and (b) 82.6 ± 1.3% (equivalent to ~625 and ~25 000 ppm, respectively, of water vapor at 1 atm and 25 °C). As shown in the figure, the sensors exhibited increasing signals upon exposure to increasing TMB concentrations, either at low RH or at high RH levels. In the case of constant RH, the high signal-to-noise ratio characterizing the response signals gives a TMB detection limit of 350 ppb. Similar behavior was observed for other VOCs as well as for the other MCNP sensors with even lower detection limits down to 100 ppb.

Figure 2 shows $\Delta R/R_b$ of a typical dodecanethiol-Au MCNP sensor exposed to air with (a) different RH levels and (b) different TMB concentrations under constant RH levels. As seen in the figure, the $\Delta R/R_b$ exhibits a linear fit with the TMB concentration (at the four different water levels) and slightly nonlinear fit with the RH concentration, characterized by an inflection point at 50% RH. The latter is a typical behavior of vapor adsorption on a porous film (classified as type II).[32] Also, the slopes of the four TMB curves were independent of the RH level, indicating that the sensitivity to the VOC is not affected by the background humidity. According to the slopes in panels a and b in Figure 2, the sensor is ~330 times more sensitive to TMB than to water, with the corresponding TMB/humidity sensitivity ratio being 1%RH/ppm$_{TMB}$. This means that the $\Delta R/R_b$ response to typical small (~3% RH) fluctuations in the humidity background is at the order of the response to low TMB concentrations (e.g., 3 ppm). Further examination of Figure 2 shows that the sensing responses were additive, i.e., the sensing response to a combination of two (or more) compounds is equal to the sum of their separate responses.[33] The rest of the MCNP sensors under analysis also showed similar characteristics for different VOCs (not shown), which should make humidity compensation potentially possible and significant.

Figure 3 shows the RH sensitivity over a period of 18 weeks for three identically fabricated NTFB-Au MCNP sensors. The RH sensitivity was estimated by exposing the sensors to two subsequent humidified air samples (61 ± 4% RH and 80 ± 4% RH), followed by obtaining the slope of the linear correlation between the two $\Delta R/R_b$ signals and the measured RHs. It can be clearly seen that the sensitivity of the chemiresistors to RH gradually decreases over time, until it reaches a plateau at ca. 40 days. The inset in Figure 3 shows the resistance of the three sensors upon exposure to the humidified air samples, at day 1 and day 122. As seen in the inset, at day 1, the sensors exhibited different baseline resistances (7.4–8.9 MΩ) and sudden resistance abruptions (about 2–3 min duration) upon exposure to humid air. Nevertheless, the more these sensors

dx.doi.org/10.1021/am2013695 | ACS Appl. Mater. Interfaces 2012, 4, 317–325

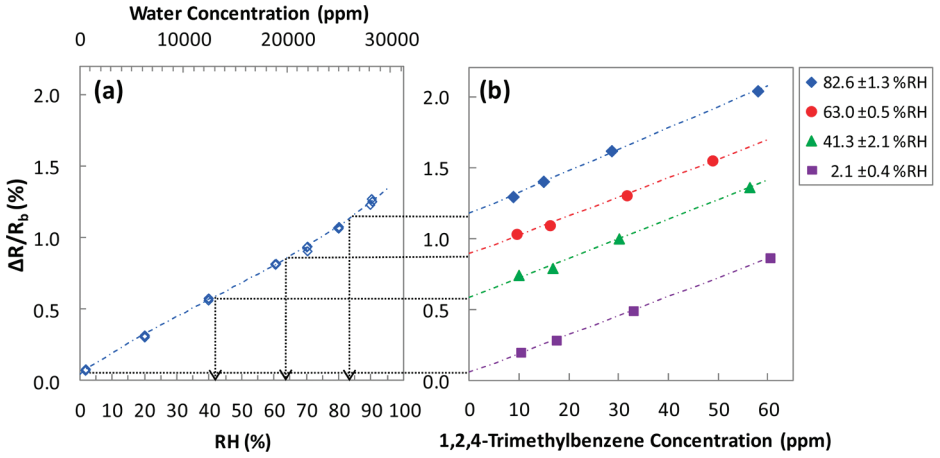

Figure 2. Normalized resistance change of the dodecanethiol-Au MCNP sensor exposed to increasing concentrations of (a) water vapor and (b) TMB with various constant RH levels (depicted in the plot's legend). The response to water was obtained from 21 exposures (seven RH levels with three repetitions). The response to TMB was obtained from 16 exposures (four RH levels with four increasing TMB concentrations). The error bars in the figure are at the length of the symbols.

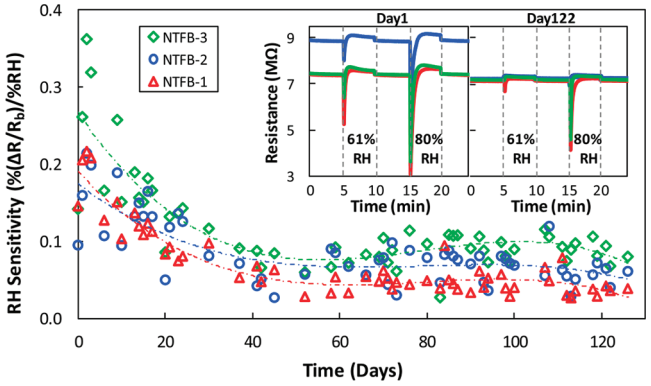

Figure 3. Correlation slopes (RH sensitivity) versus time for three identically fabricated NTFB-Au MCNP sensors. The inset shows the resistance of the three sensors upon exposure to the humidified air samples, at day 1 and day 122. The error bars in the figure are at the length of the symbols.

were used, the higher the resistance uniformity (7.1−7.2 MΩ at day 122), the weaker the response to RH, and the shorter the abruption time (about 1−2 min duration). Slight differences could be observed after this period, but they were less pronounced. Similar findings, though less substantial, were also observed for other organic capping layers, such as decanethiol and octadecanethiol.

Humidity Compensation in Mixtures of Humidity and VOCs. On the basis of the observations presented in the "Humidity Effect on the Sensing Characteristics of VOCs" part of the Results section, an approach of humidity compensation was tested as a mean for reducing the effects of highly variable humidity conditions on VOC sensing. The humidity compensation method employed is based on sensor RH calibration with an in-chamber humidity sensor, followed by postfeature extraction humidity compensation (additive compensation of the estimated sensor response to the measured humidity). In cases of short usage periods, for which the sensor's drift was <10%, a "short-term" compensation procedure was used. In cases of long usage periods, for which the sensor's drift was >10%, a "long-term" compensation procedure, which takes into account both humidity and sensitivity drift effects (see Figure 3), was implemented.

Figure 4 shows responses of the dodecanethiol-Au MCNP sensor over a period of 1 week (<5% drift) to TMB, EH, and n-octane at different concentrations, and to a mixture of three VOCs (0.85:0.96:1.00 TMB:EH:n-octane) with a RH of 2−83%. As seen in the figure, for a specific VOC concentration, the uncompensated sensing signals (closed shapes) showed varying responses at different RH levels. The higher the RH level, the higher the uncompensated sensing signal. For each specific VOC concentration, applying humidity compensation counteracted the relative effect of humidity as well as the related variances from sample to sample. This is well-expressed by the (blue) open circles presented in Figure 4, where signals at a specific VOC concentration are located at the same place in the figure. To evaluate the power for predicting VOC concentration following humidity compensation, we calculated the square of the correlation coefficient (R^2) between real and estimated VOC concentrations as a measure of how well the PLS model is likely to predict future samples (see Table 2). As expected, the PLS model showed very low R^2 values for the uncompensated signals and high values when applying the humidity compensation procedure, regardless of the large RH variance between the samples.

The effect of humidity variations was further examined by applying the short-term humidity compensation on an array of two dodecanethiol-Au MCNP sensors, two octadecanethiol-Au MCNP sensors, and one MTT-Au MCNP sensor. As seen in Figure 5, PCA analysis of the uncompensated ($\Delta R/R_b$) features has not shown any discrimination between the clusters of the different compounds. On the other hand, similar analysis applied to the compensated features showed a good separation between the various samples while showing clear concentration trajectories of the different mixtures. Figure 5b shows at the plot's center the compensated PCA signal of the lowest VOC concentration examined in this study. Gradual movement from the plot's center to the periphery indicates a gradual increase of the VOC concentration. In this way, the points closest to the graph boundaries represent the highest VOC concentration examined in this study. The classification accuracy, calculated from DFA analysis employing leave-one-out cross-validation (see "Data Analysis" part of the Experimental Section), further confirmed the significant effect of RH compensation (see Table 3).

The effect of long-term humidity compensation was examined using an array of dodecanethiol-Au MCNP, NTFB-Au

dx.doi.org/10.1021/am2013695 | ACS Appl. Mater. Interfaces 2012, 4, 317−325

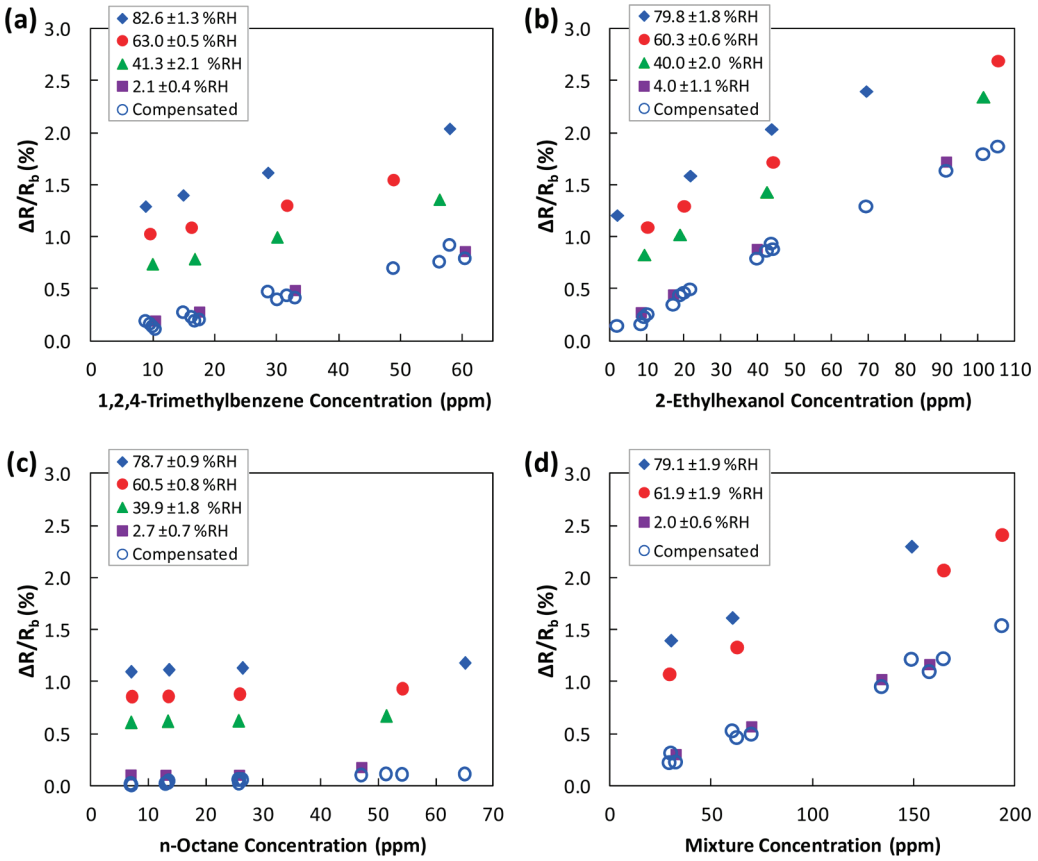

Figure 4. Uncompensated (closed shapes) and compensated (blue open circles) responses ($\Delta R/R_b$%) of a dodecanethiol-Au MCNP sensor to various concentrations of (a) TMB, (b) EH, (c) n-octane, and (d) a mixture of the three VOCs (molar ratio of 0.85 TMB:0.96 EH:1.00 n-octane) with a RH of 2–83%. The mixture concentration in the *x* axis of plot d is the total hydrocarbon concentration of the mixture. The error bars in the figures are at the length of the symbols.

Table 2. Correlation Coefficient (R^2) between Real and Predicted VOC Concentrations of Each VOC Experiment Presented in Figure 4, as Obtained from PLS Analysis of the Uncompensated and Compensated Responses of the Dodecanethiol-Au MCNP Sensor

	R^2 between real and predicted VOC concentrations			
	1,2,4-trimethylbenzene	2-ethylhexanol	n-octane	mixture
uncompensated	0.210	0.662	0.026	0.459
compensated	0.963	0.995	0.912	0.970

MCNP, MBA-Au MCNP, MTT-Au MCNP (MTT-Au NP) sensors, exposed recurrently over a period of 18 weeks to a sequence of three different samples: air with 40 ± 8 ppm EH and two humidified air samples with moderate and high water vapor contents (~61 and ~80% RH, respectively). The RH mean and standard deviation of the three air sample classes and the combined class of humidified air samples are listed in Table 4. As seen in Figure 6a, the PCA plot extracted from the uncompensated signals showed that the EH air mixtures, as well as the humidified air samples, are substantially scattered and overlap one another, making air with no EH and air with ~40 ppm EH practically indistinguishable. In contrast, the PCA plots of the compensated responses yielded well-defined and well-separated clusters of EH in the PC1 axis (accounting for 89 and 95% of the data variance for the short-term and long-term compensated signals, respectively); see Figure 6b,c.

Table 4 summarizes a statistical comparison between the three data sets (uncompensated, short-term and long-term compensated signals). Evaluation of the table shows that the long-term RH compensation is superior to the short-term method, as expressed by reduced ratios between the PC1 standard deviation and the PC1 standard deviation of the uncompensated data, for all classes. In addition, the separation between the PC1 means of the 40 ppm EH samples and humidified air samples were further increased by implementation of the long-term method. It is also evident that the larger the variance in humidity, the more substantial the reduction in scattering as a result of humidity compensation. This is well represented by the decrease in the PC1 standard deviation ratio with increasing RH standard deviation. On the other hand, one can expect that the larger the inherent class variance unrelated to humidity (e.g., VOC composition/concentration variance), the less substantial the scattering reduction following humidity compensation. Therefore, the relatively high PC1 standard deviation ratios of the 40 ppm EH class can be explained by both the low RH standard deviation (±2.8%) and the variance in EH concentration (standard deviation of ±8 ppm).

Humidity Compensation in Breath Analysis of Cancer States. The RH compensation method was applied in a clinical trial aiming for the detection of prostate cancer (PC) and breast cancer (BC), for which we have previously identified tentative volatile biomarkers in exhaled breath using a GC-MS technique – see ref 28 for more details on the VOCs

dx.doi.org/10.1021/am2013695 | ACS Appl. Mater. Interfaces 2012, 4, 317–325

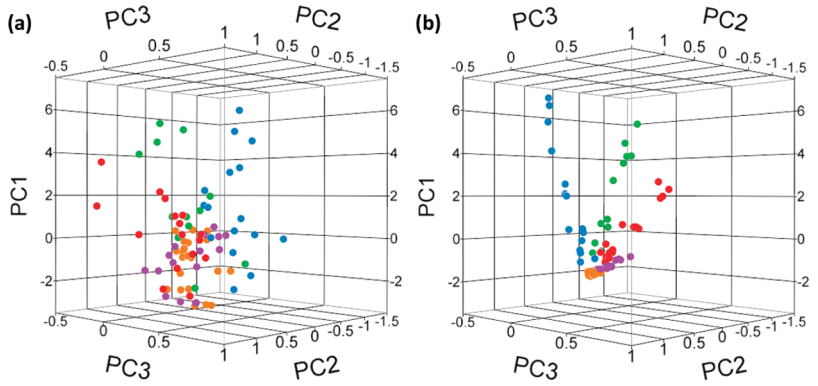

Figure 5. PCA of (a) RH uncompensated and (b) RH compensated signals for an array of two dodecanethiol-Au MCNP sensors, two octadecanethiol-Au MCNP sensors, and one 4-methoxy-α-toluenethiol-Au MCNP sensor, exposed to air with: water vapor (orange circles); binary mixtures of water vapor and EH (blue circles); water vapor and TMB (red circles); water vapor and octane (purple circles); quadruplet mixtures of water vapor, EH, TMB, and n-octane (green circles). The water vapor concentration was varied systematically between 2.1 ± 0.4% and 82.6 ± 1.3% RH, whereas the VOC concentration of the binary air mixtures was varied systematically between approximately 10 and 110 ppm, and the total VOC concentration of the quadruplet air mixtures was varied systematically between 25 and 190 ppm. For panel b, gradual movement from the plot's center to the periphery indicates a gradual increase in the VOC concentration.

Table 3. Discrimination Accuracy for the Different Air Mixtures, as Obtained from DFA of PC1, PC2, and PC3 of the Uncompensated and Compensated Responses Presented in Figure 5

	discrimination accuracy of DFA analysis (%)					
	1,2,4-trimethylbenzene	2-ethylhexanol	n-octane	mixture	water	total accuracy
uncompensated	58	83	42	67	67	64
compensated	67	92	75	83	90	83

Table 4. Statistical Data for the Different Air Sample Classes of the Long Term Sensing Experiment

			PC1 standard deviation ratio[a]		
mixture class	%RH mean	%RH std dev	uncompensated	compensated (short)	compensated (long)
40 ppm EH	6.8	2.8	1	0.96	0.69
61% RH	61.3	4.3	1	0.56	0.38
80% RH	79.5	4.5	1	0.43	0.28
humidified air	70.4	10.2	1	0.36	0.23
PC1 Δmean[b]			1.49	4.05	4.14

[a]Ratio between the PC1 standard deviation of a given class and the uncompensated PC1 standard deviation of the same class. [b]Difference between the PC1 means of the 40 ppm EH samples and humidified air samples.

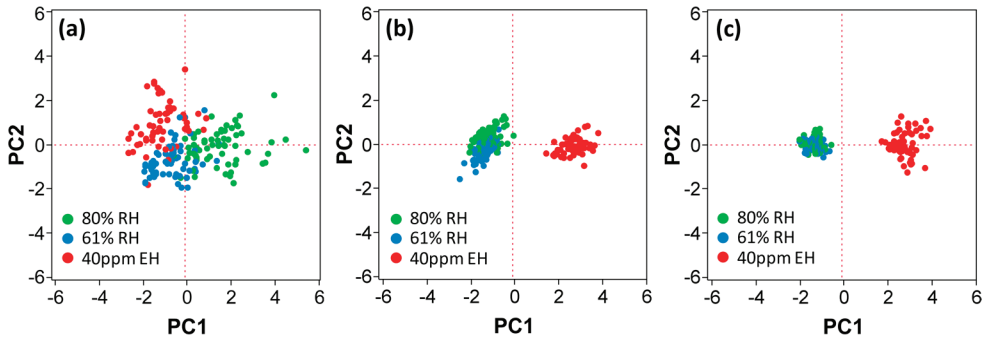

Figure 6. PCA of (a) uncompensated, (b) short-term compensated, and (c) long-term compensated responses of four Au MCNP sensors sequentially exposed over a period of 18 weeks to air samples with 40 ± 8 ppm of EH (red closed circles) and two humidified airflows with moderate RH (~61%, blue closed circles) and high RH (~80%, green closed circles). The RH mean and standard deviation of the three air sample classes and the combined class of the two humidified air samples are listed in Table 4.

characterizing each cancer state. The breath VOCs are generated by the cellular biochemical processes of the body or are absorbed from the environment through ingestion, inhalation, or through skin contact. These processes may cause specific VOCs to be emitted into the blood and, subsequently, into the alveolar exhaled breath through exchange via the lungs, generating VOC breath patterns that represent clinical states.

An array of hexanthiol-Au MCNP, *tert*-dodecanethiol-Au MCNP, 2-ethylhexanethiol-Au MCNP, (2-mercaptobenzyl alcohol)-Au MCNP, 3-methyl-1-butanethiol-Au MCNP, butanethiol-Au

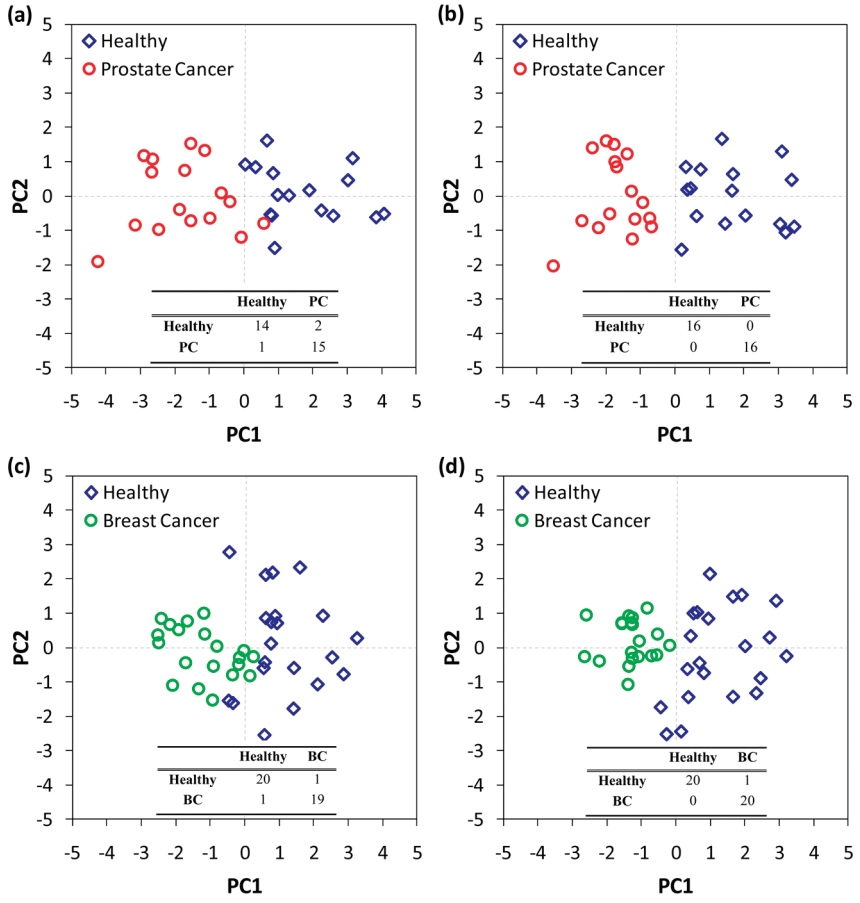

Figure 7. PCA representations of breath analysis results for a PC trial (a) without and (b) with RH compensation, and for a BC trial (c) without and (d) with RH compensation.

MCNP, and octadecylamine-Au MCNP sensors was exposed to breath samples of PC, BC, and healthy control volunteers over a period of 4 weeks (see Table 1 for a summary of the clinical characteristics of the tested groups). Following the exposure procedure, the sensing signals obtained were compensated for the RH effect, using the previously discussed approaches. The RH mean and standard deviation of the PC breath samples, as measured in-chamber during breath analysis, were 67 and 11%, respectively, and for the BC trial, 73 and 8%. Figure 7 shows a PCA representation of the sensor array breath analysis results for the PC and BC trials. As seen in the figure, the dispersion of the different clusters was reduced after the RH compensation, improving the discrimination between the healthy and the cancer groups. The classification accuracy, according to DFA analysis, based on leave-one-out cross-validation, was also improved as a consequence of RH compensation.[34] The numbers of correct and incorrect sample classifications are listed in the confusion matrixes incorporated in Figure 7. From this we can extract 94% sensitivity and 87% specificity for PC and 95% sensitivity and 95% specificity for BC using the uncompensated responses. Applying RH compensation showed improved classification values, expressed by 100% sensitivity and 100% specificity for PC and 100% sensitivity and 95% specificity for BC.

DISCUSSION

As presented in the "Humidity Compensation in Mixtures of Humidity and VOCs" part of the Results section, humidity compensation substantially improved the accuracy of VOC concentration estimation and VOC classification in synthetic mixtures. Nonetheless, the efficiency of humidity compensation varied from one mixture type to another, showing the greatest accuracy improvement for octane followed by TMB and EH. This is probably related to the lower VOC/humidity sensitivity ratio of the sensor array for octane. In addition, when considering the results presented in the "Humidity Compensation in Breath Analysis of Cancer States" part of the Results section, the humidity compensation improved the discrimination between the clusters of the synthetic samples more than that in breath samples. The reasons for this discrepancy are explained below.

The impact of humidity compensation in breath analysis is limited by a number of factors. First, the reduction in pattern variance following RH compensation is smaller when the RH variance between samples is small. This might explain the more significant scattering reduction in the case of the synthetic samples presented in Figure 5 and Table 3 (with RH standard deviation of 30%), versus the breath samples (with RH standard deviation of 10%). Second, the larger the VOC variance between samples, the less substantial the reduction due to humidity compensation. While very good control over the VOC content could be achieved in synthetic samples, this is not necessarily the case in breath samples. VOC variance exists between breath samples even when dealing with homogeneous populations sharing similar clinical backgrounds. Generally speaking, exhaled breath samples contain nitrogen, oxygen, carbon dioxide, and a spectrum of thousands of VOCs that

dx.doi.org/10.1021/am2013695 | ACS Appl. Mater. Interfaces 2012, 4, 317–325

appear in ppb levels with a total hydrocarbon composition in the ppm level. A major part of the VOC spectrum changes from one person to another while the rest of the VOCs could be found in all breath samples collected from a given population or group. As an illustrative example, a typical population of breath samples might contain between 1000 to 3000 different VOCs in total. However, the number of common VOCs that might be found in the breath of all patients could range from a few to tens of VOCs only.[10,28,30] The variance of such compounds within a breath sample population greatly varies, ranging, for example, between 0.01−1.4 ppb for hexanal, and 0.6−1582 ppb for formaldehyde (see ref 13) or 2−300 ppb for isoprene and 100−3000 ppb for acetone (see ref 12). The nature of the breath samples, therefore, implies that following humidity compensation, the remaining VOC related signal dispersion can even be enhanced if the responses of the MCNP sensors to small polar VOCs and water molecules are not additive. This could be the result of competitive adsorption due to water/VOC chemical similarity. Breath VOCs with such characteristics, such as 2-butanone, 1-propanol, ethanol, and acetone, were also found in our GC-MS analysis of breath samples from the PC, BC, and healthy control groups (see ref 12). Following these possible limitations, the use of RH compensation as a mean of reducing humidity related effects in breath analysis applications needs to be further studied, with respect to the VOC types and the concentration ranges it applies to, and verified in a larger clinical trial.

SUMMARY AND CONCLUSIONS

We have studied the effect of humidity on arrays of MCNP chemiresistors used to analyze VOCs in humid environments. This was done by evaluating the influence of humidity compensation on the VOC sensing capabilities of the sensor arrays to synthetic air mixtures as well as to complex real-world samples. In the case of the synthetic samples, a combination of large RH variance, controlled VOC composition and the additive nature of the MCNP sensor responses resulted in significant reductions in pattern dispersion following RH compensation. In the complex case of breath analysis, the reduction in pattern dispersion was less significant than that of synthetic samples. This is probably because: (i) the RH variance was smaller than that in the synthetic samples; (ii) the VOC composition in the breath samples is less controlled than in the synthetic samples; and (iii) the responses to small polar VOCs and water are not necessarily additive. In consequence, the implementation of humidity compensation for eliminating the distorting effects of humidity in breath analysis applications needs further study. A study into the validity range of humidity compensation, with respect to RH and VOC concentrations as well as temperature, is underway and will be published elsewhere. Ultimately, advances in this field could help in the development of a cost-effective, low-power method for widespread detection of VOCs in real-world applications, not only for breath analysis, but also for environmental, security, and food applications.

AUTHOR INFORMATION

Corresponding Author

*E-mail: hhossam@technion.ac.il.

ACKNOWLEDGMENTS

The research leading to these results has received funding from the FP7's ERC grant under DIAG-CANCER (grant agreement 256639) and is supported by the Alfred-Mann Institute of the Technion. We acknowledge Zvika Palkovich and Alaa Shiban for their assistance in programming, and Ms. Nisreen Shehada and Dr. Roxolyana Abdah-Bortnyak for their assistance in breath collection (Technion−IIT). H.H. is a Knight of the Order of Academic Palms.

REFERENCES

(1) Haick, H. *J. Phys. D* **2007**, *40*, 7173−7186.
(2) Tisch, U.; Haick, H. *MRS Bull.* **2010**, *35*, 797−803.
(3) Tisch, U.; Haick, H. *Rev. Chem. Eng.* **2010**, *26*, 171−179.
(4) Chow, E.; Muller, K. H.; Davies, E.; Raguse, B.; Wieczorek, L.; Cooper, J. S.; Hubble, L. J. *J. Phys. Chem. C* **2010**, *114*, 17529−17534.
(5) Zhang, H.-L.; Evans, S. D.; Henderson, J. R.; Miles, R. E.; Shen, T.-H. *Nanotechnology* **2002**, *13*, 439−444.
(6) Joseph, Y.; Guse, B.; Vossmeyer, T.; Yasuda, A. *J. Phys. Chem. C* **2008**, *112*, 12507−12514.
(7) Wilson, A.; Baietto, M. *Sens. Actuators, B* **2009**, *9*, 5099−5148.
(8) Guo, J.; Pang, P.; Cai, Q. *Sens. Actuators, B* **2007**, *120*, 521−528.
(9) Joseph, Y.; Guse, B.; Yasuda, A.; Vossmeyer, T. *Sens. Actuators, B* **2004**, *98*, 188−195.
(10) Buszewski, B.; Kesy, M.; Ligor, T.; Amann, A. *Biomed. Chromatogr.* **2007**, *21*, 553−566.
(11) Risby, T. H.; Solga, S. F.; *Appl. Phys. B* **2006**, *85*, 421−426.
(12) Bajtarevic, A.; Ager, C.; Pienz, M.; Klieber, M.; Schwarz, K.; Ligor, M.; Ligor, T.; Filipiak, W.; Denz, H.; Fiegl, M.; Hilbe, W.; Weiss, W.; Lukas, P.; Jamnig, H.; Hackl, M.; Haidenberger, A.; Buszewski, B.; Miekisch, W.; Schubert, J.; Amann, A. *BMC Cancer* **2009**, *348*, 1−16.
(13) Fuchs, P.; Loeseken, C.; Schubert, K. J.; Miekisch, W. *Int. J. Cancer* **2010**, *126*, 2663−2670.
(14) Song, G.; Qin, T.; Liu, H.; Xu, G. B.; Pan, Y. Y.; Xiong, F. X.; Gu, K. S.; Sun, G. P.; Chen, Z. D. *Lung Cancer* **2010**, *67*, 227−231.
(15) Patel, S. V.; Jenkins, M. W.; Hughes, R. C.; Yelton, W. G.; Ricco, A. J. *Anal. Chem.* **2000**, *72*, 1532−1542.
(16) Peng, G.; Trock, E.; Haick, H. *Nano Lett.* **2008**, *8*, 3631−3635.
(17) Holmberg, M.; Davide, F. A. M.; DiNatale, C.; D'Amico, A.; Winquist, F.; Lundstrom, I. *Sens. Actuators, B* **1997**, *42*, 185−194.
(18) Rock, F.; Barsan, N.; Weimar, U. *Chem. Rev.* **2008**, *108*, 705−725.
(19) Groves, W. A.; Zellers, E. T. *Ann. Occup. Hyg.* **2001**, *45*, 609−623.
(20) Dovgolevsky, E.; Tisch, U.; Haick, H. *Small* **2009**, *5*, 1158−1161.
(21) Dovgolevsky, E.; Konvalina, G.; Tisch, U.; Haick, H. *J. Phys. Chem. C* **2010**, *114*, 14042−14049.
(22) Peng, G.; Tisch, U.; Haick, H. *Nano Lett.* **2009**, *9*, 1362−1368.
(23) Zilberman, Y.; Ionescu, R.; Feng, X.; Mullen, K.; Haick, H. *ACS Nano* **2011**, *5*, 6743−6753.
(24) Zilberman, Y.; Tisch, U.; Pisula, W.; Feng, X.; Müllen, K.; Haick, H. *Langmuir* **2009**, *25*, 5411−5416.
(25) Zilberman, Y.; Tisch, U.; Shuster, G.; Pisula, W.; Feng, X.; Müllen, K.; Haick, H. *Adv. Mater.* **2010**, *22*, 4317−4320.
(26) Garg, N.; Mohanty, A.; Lazarus, N.; Schultz, L.; Rozzi, T. R.; Santhanam, S.; Weiss, L.; Snyder, J. L.; Fedder, G. K.; Jin, R. *Nanotechnology* **2010**, *21*, 405501.
(27) Dovgolevsky, E.; Haick, H. *Small* **2008**, *4*, 2059−2066.
(28) Peng, G.; Hakim, M.; Broza, Y. Y.; Billan, S.; Abdah-Bortnyak, R.; Kuten, A.; Tisch, U.; Haick, H. *Br. J. Cancer* **2010**, *103*, 542−551.
(29) Hakim, M.; Billan, S.; Tisch, U.; Peng, G.; Dvrokind, I.; Marom, O.; Abdah-Bortnyak, R.; Kuten, A.; Haick, H. *Br. J. Cancer* **2011**, *104*, 1649−1655.
(30) Peng, G.; Tisch, U.; Adams, O.; Hakim, M.; Shehada, N.; Broza, Y. Y.; Billan, S.; Abdah-Bortnyak, R.; Kuten, A.; Haick, H. *Nature Nanotechnol.* **2009**, *4*, 669−673.
(31) Geladi, P.; Kowalski, B. R. *Anal. Chim. Acta* **1986**, *185*, 1−17.
(32) Huang, H.; Haghighat, F.; Blondeau, P. *Indoor Air* **2006**, *16*, 236−247.

(33) Severin, E. J.; Doleman, B. J.; Lewis, N. S. *Anal. Chem.* **2000**, *72*, 658−668.

(34) To reduce the risk of overfitting only three sensors were used for the DFA, as the test populations are relatively small and, unlike PCA, DFA is a supervised learning method in which the data set classes are used to achieve the best discrimination.